
Regulation of closely juxtaposed proto-oncogene *c-fms* and *HMGXB3* gene expression by mRNA 3' end polymorphism in breast cancer cells

HO-HYUNG WOO¹ and SETSUKO K. CHAMBERS^{1,2}

¹The University of Arizona Cancer Center, Tucson, Arizona 85724, USA

²Department of Obstetrics and Gynecology, College of Medicine, The University of Arizona, Tucson, Arizona 85724, USA

ABSTRACT

Sense-antisense mRNA pairs generated by convergent transcription is a way of gene regulation. *c-fms* gene is closely juxtaposed to the *HMGXB3* gene in the opposite orientation, in chromosome 5. The intergenic region (IR) between *c-fms* and *HMGXB3* genes is 162 bp. We found that a small portion (~4.18%) of *HMGXB3* mRNA is transcribed further downstream, including the end of the *c-fms* gene generating antisense mRNA against *c-fms* mRNA. Similarly, a small portion (~1.1%) of *c-fms* mRNA is transcribed further downstream, including the end of the *HMGXB3* gene generating antisense mRNA against the *HMGXB3* mRNA. Insertion of the strong poly(A) signal sequence in the IR results in decreased *c-fms* and *HMGXB3* antisense mRNAs, resulting in up-regulation of both *c-fms* and *HMGXB3* mRNA expression. miR-324-5p targets *HMGXB3* mRNA 3' UTR, and as a result, regulates *c-fms* mRNA expression. HuR stabilizes *c-fms* mRNA, and as a result, down-regulates *HMGXB3* mRNA expression. UALCAN analysis indicates that the expression pattern between *c-fms* and *HMGXB3* proteins are opposite in vivo in breast cancer tissues. Together, our results indicate that the mRNA encoded by the *HMGXB3* gene can influence the expression of adjacent *c-fms* mRNA, or vice versa.

Keywords: convergent transcription termination; sense-antisense RNA pairing; mRNA 3' end polymorphism; *c-fms* mRNA 3' end; *HMGXB3* mRNA 3' end

INTRODUCTION

In RNA polymerase II (RNAPII)-driven transcription elongation, termination, transcript cleavage, and release commonly occur after recognizing the poly(A) site (PAS) by the 3' end cleavage and polyadenylation (CPA) complex (West et al. 2008; Kuehner et al. 2011; Proudfoot 2016). Cleavage by CPA releases the nascent transcript, which becomes polyadenylated at the 3' end (Proudfoot 1989). When more than one PAS is present, alternative polyadenylation occurs.

Transcription termination can also occur anywhere from the 3' end of the mRNA by readthrough transcription (Proudfoot 1989; Dye and Proudfoot 1999; Richard and Manley 2009), which generates the mRNA 3' end polymorphism (de Klerk and 't Hoen 2015; Kainov et al. 2016; Nourse et al. 2020). In yeast, various transcript boundaries are present (Gullerova and Proudfoot 2008; Pelechano et al. 2013).

In the case of a convergent gene pair, RNAPII molecules in the transcription elongation complex collide head-to-

head and stop transcription (Hobson et al. 2012). In head-to-head collision, RNAPII molecules may also bypass one another, generating sense-antisense transcript pairs overlapping at the 3' end (Ma and McAllister 2009). In humans, over 20% of transcripts may form sense-antisense pairs, in which most antisense transcripts (i.e., *cis*-encoded natural antisense, *cis*-NAT) are generated from the opposite strand of the same genomic locus of the sense strand (Yelin et al. 2003; Chen et al. 2004; Zhang et al. 2006).

Natural antisense transcripts (NATs) are prevalent in human cells (Zhang et al. 2006; Pelechano and Steinmetz 2013). *cis*-NATs have perfect sequence complementary to the sense transcripts. *cis*-NATs can be derived from tail-to-tail (3' to 3') to their relative orientation (Lapidot and Pilpel 2006). NATs are proposed to be involved in several regulatory mechanisms. NAT can interfere with sense transcription by collision of two RNAPII complexes. NAT can also mask sense mRNA and hinder protein-RNA interaction

© 2021 Woo and Chambers This article is distributed exclusively by the RNA Society for the first 12 months after the full-issue publication date (see <http://rnajournal.cshlp.org/site/misc/terms.xhtml>). After 12 months, it is available under a Creative Commons License (Attribution-NonCommercial 4.0 International), as described at <http://creativecommons.org/licenses/by-nc/4.0/>.

Corresponding author: hwoo@u.arizona.edu

Article is online at <http://www.majournal.org/cgi/doi/10.1261/rna.078749.121>.

in the cytoplasm, resulting in translation inhibition and RNA decay. Interaction of 3' overlapping mRNAs promotes no-go-decay in the cytoplasm (Sinturel et al. 2015).

In RNA interference (RNAi), dsRNA formed by convergent transcription is processed to generate siRNAs, which are incorporated into the RNAi-induced silencing (RISC) complex for posttranscriptional gene silencing (PTGS) by inducing mRNA decay and translational repression (Borsani et al. 2005; Kim and Nam 2006; Carthew and Sontheimer 2009; Pelechano and Steinmetz 2013). In the nucleus, siRNA derived from dsRNA by convergent transcription is involved in transcriptional gene silencing (TGS) (Gullerova and Proudfoot 2012). In TGS, siRNA-induced transcriptional silencing (RITS) complex targets homologous gene loci, which in turn induce heterochromatin formation resulting in gene silencing (Buhler and Moazed 2007). In this aspect, TGS and PTGS are proposed to cooperate for gene silencing (Faghihi and Wahlestead 2009; Werner and Sayer 2009).

Aberrant mRNA 3' end cleavage and processing are known to associate with diseases including cancer (Danckwardt et al. 2008; Di Giammartino et al. 2011; Ogorodnikov et al. 2016; Nourse et al. 2020). Both point mutations in PAS as well as mutations in CPA complexes have resulted in aberrant 3' end processing and pathogenesis.

Here, we describe gene regulation by *cis*-NATs generated from a convergent gene pair consisting of the proto-oncogene *c-fms* and the *HMGXB3* gene. The proto-oncogene *c-fms*, which encodes the receptor tyrosine kinase and a sole receptor for CSF-1, is expressed by the tumor epithelium in several human epithelial cancers (Kacinski et al. 1988, 1990, 1991). An elevated level of *c-fms* is associated with poor prognosis (Chambers et al. 1997; Maher et al. 1998). Activated (phosphorylated) *c-fms* protein in breast and ovarian cancer is present in over 50% of tumors (Flick et al. 1997; Toy et al. 2001). In breast cancer, interaction of *c-fms* bearing tumor associated macrophages in breast tissues promotes malignant transformation (Lin et al. 2001). HuR is a member of the Elav/Hu family of RNA-binding proteins and plays a supportive role for *c-fms* in breast cancer progression by binding a pyrimidine-rich sequence in its mRNA 3' UTR, thus regulating its expression (Woo et al. 2009).

HMGXB3 belongs to a high-mobility group binding protein 3 family. Currently, there is limited information about *HMGXB3* at the molecular level. However, *HMGXB3* is known to be involved in cell proliferation and migration (Guo et al. 2016; Sing et al. 2019). Knockdown of *HMGXB3* inhibits cell proliferation and reduces migration in gastric cancer cells (Guo et al. 2016) and non-small cell lung cancer cells (Song et al. 2019). miR-324-5p targets *HMGXB3* mRNA 3' UTR and down-regulates its expression (Sun et al. 2017).

We report here that the proto-oncogene *c-fms* and *HMGXB3* are a convergent gene pair with a 162 bp inter-

genic region between their 3' ends. They each generate mRNAs with extended 3' ends which are *cis*-antisense RNA against the 3' end of their pair mRNA. Expression of both genes regulate each other by sense-antisense RNA pairing, which may be self-regulatory circuits to regulate their own expression.

RESULTS

c-fms and *HMGXB3* mRNA 3' end polymorphisms are derived from extended transcription termination

Both *c-fms* and *HMGXB3* genes are closely juxtaposed in chromosome 5. The intergenic region between two genes is 162 bp (Fig. 1A). Since both genes are closely located in the opposite orientation, we checked the presence of mRNA 3' end extension generated by readthrough convergent transcription termination. For northern blot analysis, strand-specific antisense RNA probes 1 through 4 were generated to detect either *c-fms* or *HMGXB3* mRNA with 3' end extension (Supplemental Fig. S1). Northern blot analysis indicates that *HMGXB3* mRNA is detected by strand-specific antisense RNA probe 1 generated from the *HMGXB3* mRNA coding region in 1 h exposure (Fig. 1B). In addition, *HMGXB3* mRNA with 3' end extension is also detected by strand-specific antisense RNA probe 2 generated from the *c-fms* mRNA 3' UTR in 96 h exposure (Fig. 1B). Strand-specific antisense RNA probe 2 cannot detect *c-fms* mRNA, since it is sense *c-fms* RNA.

Northern blot analysis also indicates that *c-fms* mRNA is detected by strand-specific antisense RNA probe 3 generated from the *c-fms* mRNA coding region in 1 h exposure (Fig. 1C). In addition, *c-fms* mRNA with 3' end extension is also detected by strand-specific antisense RNA probe 4 generated from the *HMGXB3* mRNA 3' UTR in 96 h exposure (Fig. 1C). Strand-specific antisense RNA probe 4 cannot detect *HMGXB3* mRNA, since it is sense *HMGXB3* RNA.

This indicates that a small portion of *c-fms* and *HMGXB3* mRNAs with 3' end extensions are present, since weak signals are detected by strand-specific antisense RNA probes 2 and 4 in 96 h exposure.

Mapping and quantification of *c-fms* and *HMGXB3* mRNAs with 3' end extensions

To map the 3' end extensions of *c-fms* and *HMGXB3* mRNAs, we did RT-PCR with strand-specific primers and poly-(A)⁺-RNA (Fig. 2A). Reverse transcription was performed with strand-specific primers from multiple different locations of *c-fms* and *HMGXB3* mRNAs (Fig. 2A; Supplemental Fig. S2A,B; Supplemental Table S1). The 3' end of *HMGXB3* mRNA is extended up to 578 nt inside of the *c-fms* mRNA 3' UTR (i.e., up to *c-fms* mRNA +3411nt). The 3' end of *c-fms* mRNA is extended up to 939 nt inside of the *HMGXB3* mRNA 3' UTR (i.e., up to *HMGXB3* mRNA +4320 nt).

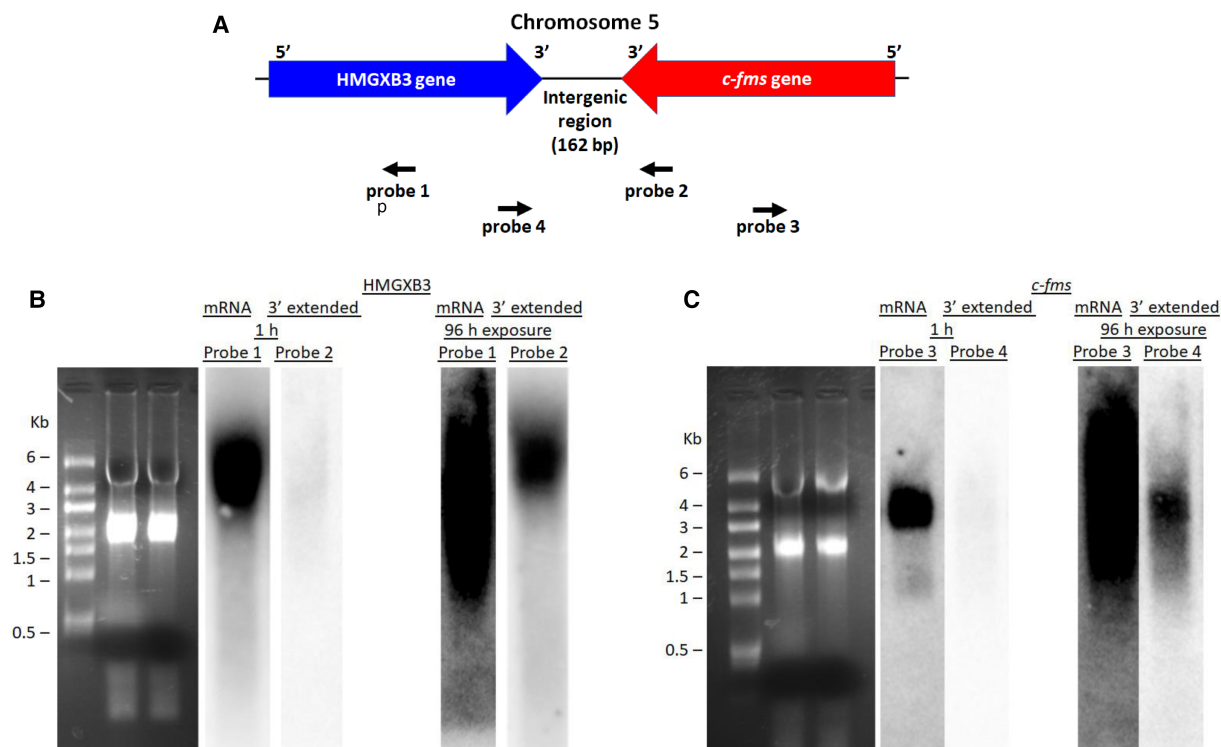


FIGURE 1. *c-fms* and *HMGXB3* mRNA 3' end polymorphism. (A) Both *HMGXB3* gene and *c-fms* gene are closely juxtaposed in chromosome 5. The intergenic region is 162 bp. ^{32}P -labeled strand-specific antisense RNA probe 1 derived from the *HMGXB3* mRNA coding region detects *HMGXB3* mRNA. ^{32}P -labeled strand-specific antisense RNA probe 2 derived from the 3' end of *c-fms* mRNA detects 3' end extended *HMGXB3* mRNA. ^{32}P -labeled strand-specific antisense RNA probe 3 derived from *c-fms* mRNA coding region detects *c-fms* mRNA. ^{32}P -labeled strand-specific antisense RNA probe 4 derived from the 3' end of *HMGXB3* mRNA detects 3' end extended *c-fms* mRNA. Detailed description of probe generation is in Supplemental Figure S1. (B) Northern blot shows *HMGXB3* mRNA and *HMGXB3* mRNA with 3' end extension. *HMGXB3* mRNA is detected in 1 h exposure. In contrast, *HMGXB3* mRNA with 3' end extension is detected in 96 h exposure. (C) Northern blot shows *c-fms* mRNA and *c-fms* mRNA with 3' end extension. *C-fms* mRNA is detected in 1 h exposure. In contrast, *c-fms* mRNA with 3' end extension is detected in 96 h exposure.

For further quantification, we measured *c-fms* and *HMGXB3* total mRNAs and also 3' end extensions by strand-specific qRT-PCR (described in Supplemental Fig. S2C,D). Quantification of both mRNAs and the 3' end extensions indicates that *c-fms* mRNA with the 3' end extension is ~4.1% of total *c-fms* mRNA (Fig. 2B; Supplemental Fig. S2E). Similarly, *HMGXB3* mRNA with the 3' end extension is ~1.1% of total *HMGXB3* mRNA (Fig. 2C; Supplemental Fig. S2F).

We conclude that a small portion of *c-fms* and *HMGXB3* mRNAs with the 3' end extensions are generated by read-through convergent transcription termination. These *c-fms* and *HMGXB3* mRNAs with the 3' end extensions also have poly-(A)⁺ tails, since poly-(A)⁺-RNA was used for mapping (Fig. 2A).

Introduction of strong poly(A) signal sequence in the intergenic region increases both *c-fms* and *HMGXB3* expression

To block the extended transcription termination, a strong poly(A) signal sequence SV40-PA (Schek et al. 1992;

Hans and Alwine 2000) was introduced in the intergenic region (IR) in chromosome 5 via CRISPR/Cas9 (Fig. 3A). Insertion of SV40-PA was confirmed by genome PCR and sequencing (Supplemental Fig. S3A). Insertion of SV40-PA in the IR abolishes the expression of *HMGXB3* mRNA with the 3' end extension (which is antisense to the *c-fms* mRNA 3' end) (Fig. 3B Northern) thereby increasing the steady-state level of *c-fms* mRNA by 2.5-fold ($n=4$, Fig. 3E; Supplemental Fig. S3B) and protein by 2.6-fold (Fig. 3F) compared to the wild-type cells. Insertion of SV40-PA in the IR also abolishes the expression of *c-fms* mRNA with the 3' end extension (which is antisense to the *HMGXB3* mRNA 3' end) (Fig. 3C Northern) thereby increasing the steady-state level of *HMGXB3* mRNA by 1.46-fold ($n=4$, $P<0.001$, Fig. 3E; Supplemental Fig. S3C) and protein by 1.6-fold (± 0.32 , $n=4$, Fig. 3F; Supplemental Fig. S3E).

When the wild-type (WT) group in BT20 cells was compared with the SV40-PA inserted group, the half-life of *c-fms* mRNA increased from 8 h to >24 h (two-tailed t-test, $n=3$, $P<0.001$) (Fig. 3G). The half-life of *HMGXB3* mRNA also increased from 4 h to >8 h (two-tailed t-test, $n=3$, $P<0.001$) (Fig. 3H).

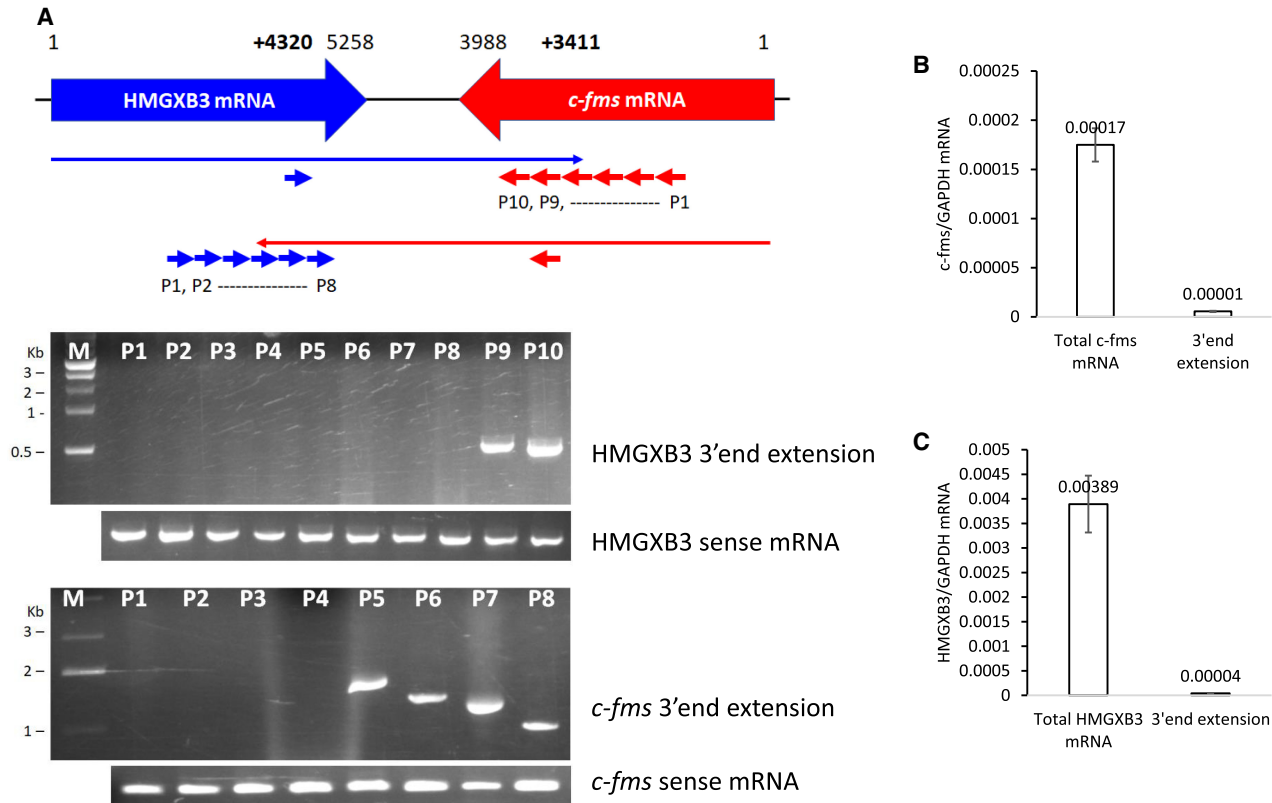


FIGURE 2. Mapping and quantification of transcripts with the 3' end extensions. (A) Mapping of 3' end extension by RT-PCR. The *HMGXB3* mRNA with the 3' end extension was reverse transcribed by 10 primers derived from the *c-fms* mRNA sequence. RT transcript was PCR amplified for mapping. The *c-fms* mRNA with the 3' end extension was reverse transcribed by eight primers derived from the *HMGXB3* mRNA sequence. RT transcript was PCR amplified for mapping. A detailed mapping strategy is described in Supplemental Figure S2. (B) qRT-PCR indicates that *c-fms* mRNA with 3' end extension is 4.1% of total *c-fms* mRNA ($n = 4$). (C) qRT-PCR indicates that *HMGXB3* mRNA with 3' end extension is 1.1% of total *HMGXB3* mRNA ($n = 4$). Detailed quantification strategy is described in Supplemental Figure S2.

These results underscore the stabilizing influence of SV40-PA insertion by down-regulating *c-fms* or *HMGXB3* mRNAs with the 3' end extensions, which serve as natural antisense RNAs.

miR-324-5p regulates *c-fms* mRNA expression via interacting with *HMGXB3* mRNA

Sun et al. (2017) reported that miR-324-5p interacts with *HMGXB3* mRNA 3' UTR. TargetScan ([http://www.targetscan.org/vert 72/](http://www.targetscan.org/vert_72/)) for prediction of miRNA targets also predicts the interaction of miR-324-5p with *HMGXB3* mRNA, but not with *c-fms* mRNA. We checked whether the interaction of miR-324-5p with *HMGXB3* mRNA influences the expression of *c-fms* mRNA. miR-324-5p mimic down-regulates the steady-state level of *HMGXB3* mRNA and up-regulates *c-fms* mRNA ($n = 4$, Fig. 4A; Supplemental Fig. S4A,B). A similar effect was also observed in their protein levels, that is, miR-324-5p mimic down-regulates *HMGXB3* protein expression and up-regulates *c-fms* protein expression (Fig. 4B; Supplemental Fig. S4C).

We studied the effects of altering *HMGXB3* mRNA levels by miR-324-5p mimic on *c-fms* mRNA half-life in BT20 cells. As shown in Figure 2C, at least part of the 3.2-fold increase in the steady-state level of *c-fms* mRNA in BT20 cells seen on miR-324-5p mimic (Fig. 4A) is due to an increase in the stability of *c-fms* mRNA (Fig. 4C). When the scramble control group in BT20 cells was compared with the miR-324-5p mimic group, the half-life of *c-fms* mRNA increased from 8 h to >24 h (two-tailed t-test, $n = 3$, $P < 0.001$). These results underscore the stabilizing influence of miR-324-5p mimic on *c-fms* mRNA. At the same time, the half-life of *HMGXB3* mRNA decreased from 4 h to <2 h (two-tailed t-test, $n = 3$, $P < 0.001$). These results also underscore the destabilizing influence of miR-324-5p mimic on *HMGXB3* mRNA (Fig. 4D).

Conversely, miR-324-5p inhibitor up-regulates the steady-state level of *HMGXB3* mRNA, and down-regulates *c-fms* mRNA ($n = 4$, Fig. 4E; Supplemental Fig. S4D,E). A similar effect was also observed in protein levels, that is, miR-324-5p inhibitor up-regulates *HMGXB3* protein expression and down-regulates *c-fms* protein expression (Fig. 4F; Supplemental Fig. S4F).

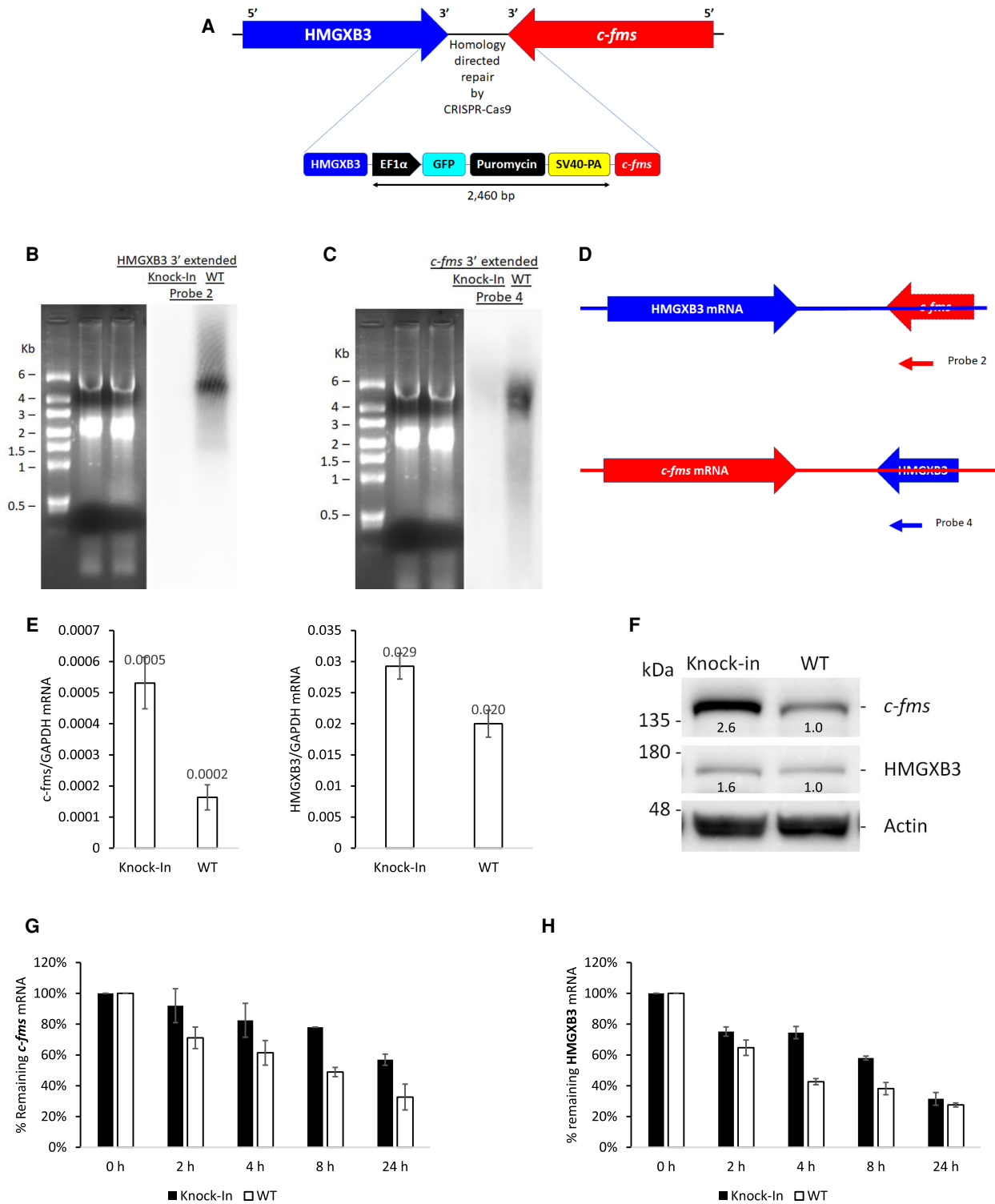


FIGURE 3. Insertion of strong poly(A) signal in the intergenic region increases the expression of both *c-fms* and *HMGXB3*. (A) SV40-PA is inserted in the intergenic region by CRISPR-Cas9. Confirmation of insertion is shown in Supplemental Figure S3. (B) SV40-PA knock-in abolishes the expression of *HMGXB3* mRNA with 3' end extension, and (C) the expression of *c-fms* mRNA with 3' end extension. Northern blot was exposed for 96 h. (D) ³²P-labeled strand-specific antisense probe 2 is derived from the *c-fms* mRNA 3' end. ³²P-labeled strand-specific antisense probe 4 is derived from *HMGXB3* mRNA 3' end. ³²P-labeled strand-specific probes 2 and 4 were synthesized as described in Supplemental Figure S1. (E) SV40-PA knock-in increases *c-fms* mRNA and *HMGXB3* mRNA (n = 4). (F) SV40-PA knock-in increases both *c-fms* protein and *HMGXB3* protein. Numbers below bands indicate band intensities scanned by ImageJ. (G) SV40-PA knock-in increases *c-fms* mRNA half-life, and (H) *HMGXB3* mRNA half-life (n = 3).

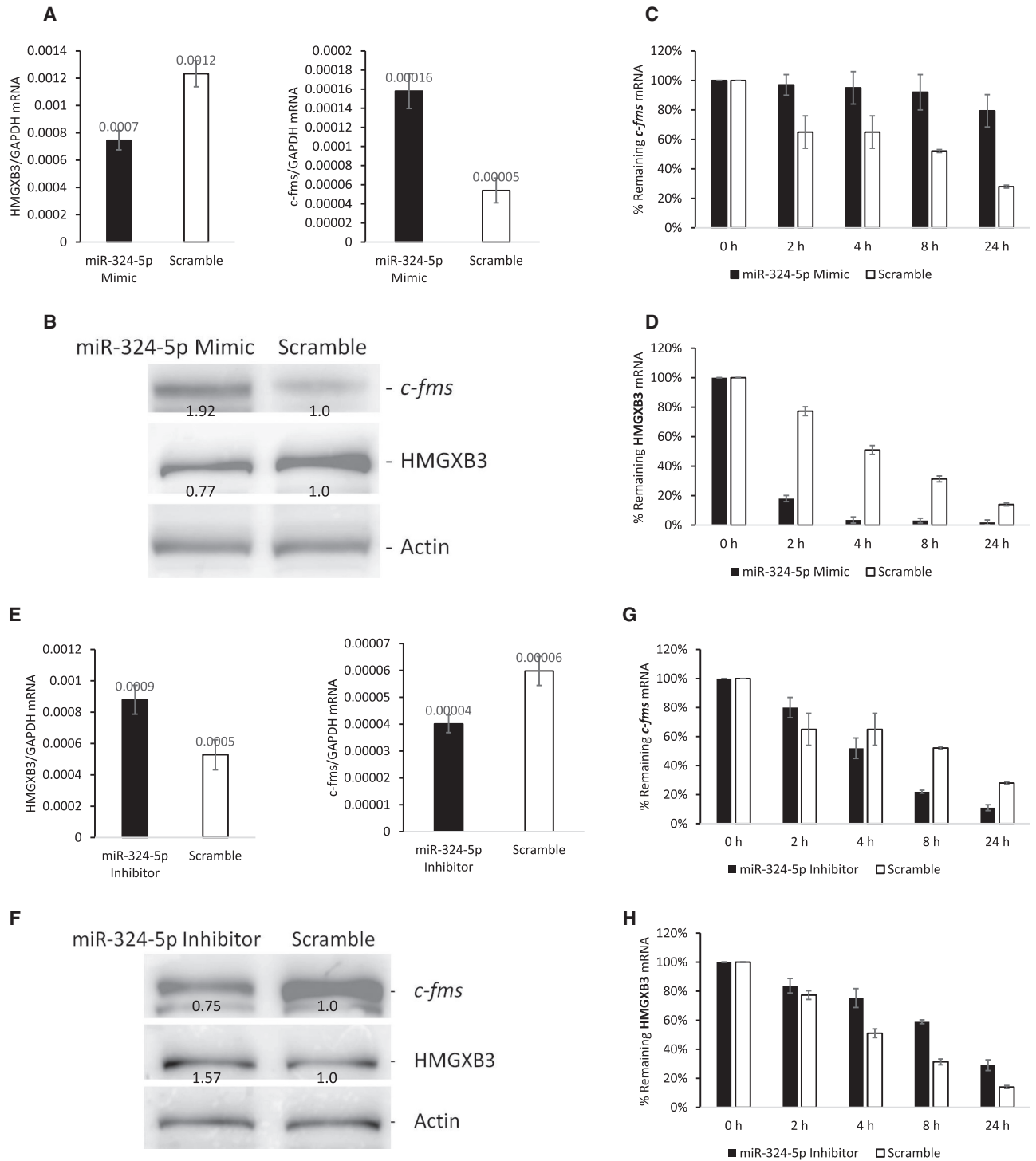


FIGURE 4. miR-324-5p regulates *c-fms* mRNA expression thru *HMGXB3* mRNA. (A) miR-324-5p mimic decreases *HMGXB3* mRNA and increases *c-fms* mRNA ($n = 4$). (B) Western analysis shows increased expression of *c-fms* protein and decreased expression of *HMGXB3* protein by miR-324-5p mimic. Numbers below bands indicate band intensities scanned by ImageJ. (C) miR-324-5p mimic increases *c-fms* mRNA half-life ($n = 3$). (D) miR-324-5p mimic decreases *HMGXB3* mRNA half-life ($n = 3$). (E) miR-324-5p inhibitor increases *HMGXB3* mRNA and decreases *c-fms* mRNA ($n = 4$). (F) Western analysis shows decreased expression of *c-fms* protein and increased expression of *HMGXB3* protein by miR-324-5p inhibitor. Numbers below bands indicate band intensities scanned by ImageJ. (G) miR-324-5p inhibitor decreases *c-fms* mRNA half-life ($n = 3$). (H) miR-324-5p inhibitor increases *HMGXB3* mRNA half-life ($n = 3$).

We also studied the effects of altering *HMGXB3* mRNA level by miR-324-5p inhibitor on *c-fms* mRNA half-life in BT20 cells. When the scramble control group in BT20 cells was compared with the miR-324-5p inhibitor group, the half-life of *c-fms* mRNA decreased from 8 h to ~4 h (two-tailed t-test, $n = 3$, $P < 0.001$) (Fig. 4G). These results underscore the destabilizing influence of miR-324-5p inhibitor on *c-fms* mRNA. At the same time, the half-life of *HMGXB3* mRNA increased from 4 h to >8 h (two-tailed t-test, $n = 3$, $P < 0.001$) (Fig. 4H). These results also underscore the stabilizing influence of miR-324-5p inhibitor on *HMGXB3* mRNA.

We conclude that miR-324-5p regulates *c-fms* mRNA expression via interacting with *HMGXB3* mRNA.

miR-324-5p targets *HMGXB3* mRNA 3' UTR, not *c-fms* mRNA 3' UTR

Since Sun et al. (2017) reported direct targeting of miR-324-5p to *HMGXB3* mRNA 3' UTR, we further verified that miR-324-5p does not also target the 3' UTR of *c-fms* mRNA. To do this, we made luciferase reporter fused with either *HMGXB3* or *c-fms* mRNA 3' UTRs (Supplemental Fig. S5A). BT20 cells were cotransfected either miR-324-5p mimic or miR-324-5p inhibitor with luciferase-3' UTR reporter plasmids bearing 3' UTR sequence

of either *c-fms* or *HMGXB3* mRNA. As expected, miR-324-5p mimic reduced the steady-state luciferase mRNA and activity of *HMGXB3* reporter plasmid ($n = 4$, Fig. 5A, B; Supplemental Fig. S5B). Conversely, the steady-state luciferase-*HMGXB3* mRNA 3' UTR and activity were increased by cotransfected with miR-324-5p inhibitor.

As shown in Figure 5C, at least part of the 2.5-fold decrease in the steady-state level of luciferase-*HMGXB3* mRNA in BT20 cells seen in the miR-324-5p mimic group (Fig. 5A) is due to a decrease in the stability of luciferase-*HMGXB3* mRNA (Fig. 5C). When the scramble control group in BT20 cells was compared with the miR-324-5p mimic group, the half-life of luciferase-*HMGXB3* mRNA 3' UTR decreased from 6 h to 4 h (two-tailed t-test, $n = 3$, $P < 0.001$). These results underscore the destabilizing influence of miR-324-5p mimic on luciferase-*HMGXB3* mRNA 3' UTR. At the same time, the half-life of luciferase-*HMGXB3* mRNA 3' UTR increased from 6 h to >8 h (two-tailed t-test, $n = 3$, $P < 0.001$) in the miR-324-5p inhibitor treatment group. These results also underscore the stabilizing influence of miR-324-5p inhibitor on luciferase-*HMGXB3* mRNA 3' UTR (Fig. 5C).

In contrast, miR-324-5p mimic increased the steady-state level of luciferase mRNA and activity of *c-fms* mRNA 3' UTR reporter plasmid ($n = 4$, Fig. 5D,E; Supplemental Fig. S5C). This increase is likely due to the

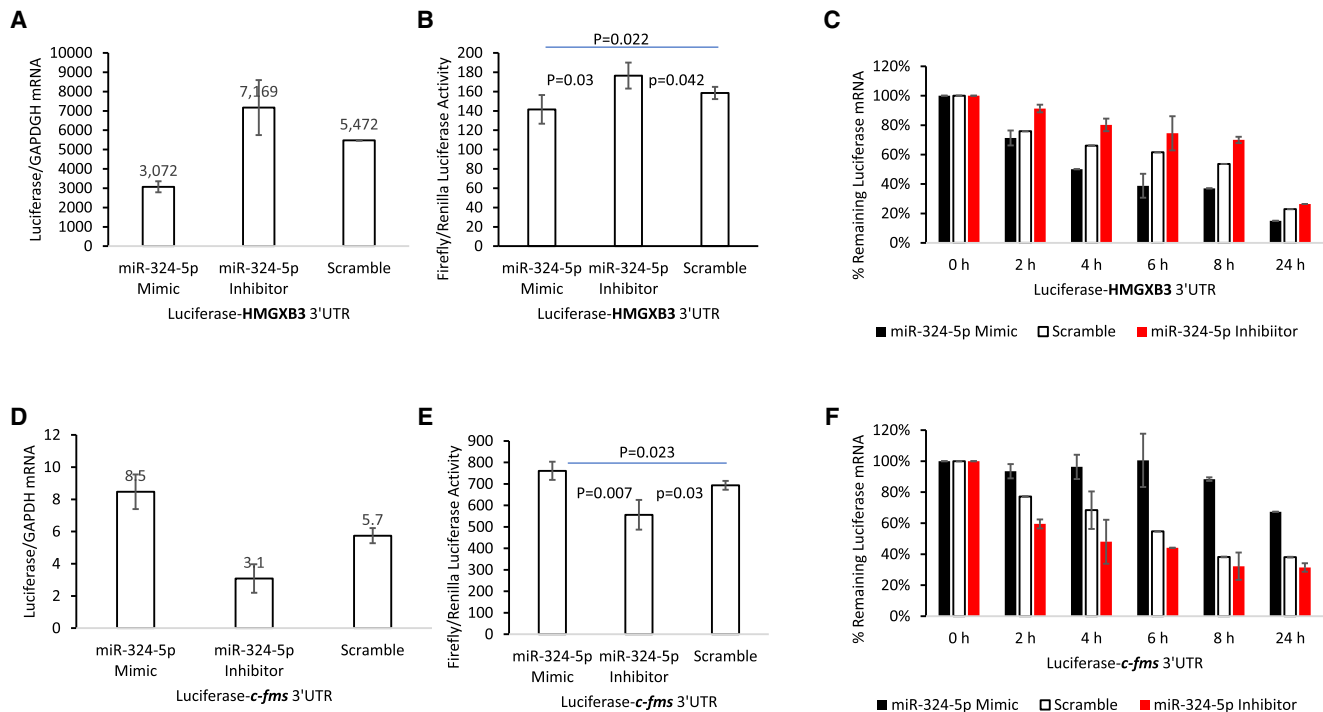


FIGURE 5. Luciferase reporter assay indicates that miR-324-5p has opposite effects on *HMGXB3* and *c-fms* expression. (A,B) miR-324-5p mimic decreases and miR-324-5p inhibitor increases luciferase-*HMGXB3* mRNA 3' UTR reporter expression ($n = 4$). (C) miR-324-5p mimic decreases (black bar) and miR-324-5p inhibitor increases luciferase-*HMGXB3* mRNA 3' UTR reporter RNA half-life (red bar) ($n = 3$). (D,E) miR-324-5p mimic increases and miR-324-5p inhibitor decreases luciferase-*c-fms* mRNA 3' UTR reporter expression ($n = 4$). (F) miR-324-5p mimic increases (black bar) and miR-324-5p inhibitor decreases luciferase-*c-fms* mRNA 3' UTR reporter RNA half-life (red bar) ($n = 3$).

decrease of the *HMGXB3* mRNA with 3' end extension (which is antisense to the *c-fms* mRNA 3' end in luciferase construct). Conversely, the steady-state luciferase-*c-fms* mRNA 3' UTR and activity were decreased by cotransfection with miR-324-5p inhibitor. This decrease is also likely due to the increase of the *HMGXB3* mRNA with 3' end extension. When the scramble control group in BT20 cells was compared with the miR-324-5p mimic group, the half-life of luciferase-*c-fms* mRNA 3' UTR increased from 6 h to >24 h (two-tailed *t*-test, $n = 3$, $P < 0.001$) (Fig. 5F). These results underscore the destabilizing influence of miR-324-5p mimic on the *HMGXB3* 3' end extended transcript. At the same time, the half-life of luciferase-*c-fms* mRNA 3' UTR decreased from 6 h to 4 h (two-tailed *t*-test, $n = 3$, $P < 0.001$) in the miR-324-5p inhibitor treatment group. These results also underscore the stabilizing influence of miR-324-5p inhibitor on the *HMGXB3* mRNA with 3' end extension.

We conclude that miR-324-5p directly targets *HMGXB3* mRNA 3' UTR, not the *c-fms* mRNA 3' UTR.

HuR up-regulates *c-fms* mRNA and down-regulates *HMGXB3* mRNA expression

We previously reported that HuR, an RNA binding protein, interacts and stabilizes *c-fms* mRNA, resulting in an increase of *c-fms* expression (Woo et al. 2009). To test whether HuR also directly associates with *HMGXB3* mRNA, IP assay was performed in BT20 cells (Fig. 6A).

Possible association of *HMGXB3* mRNA with HuR was determined by isolating RNA from the IP material and analyzing it by quantitative real-time PCR. As shown in Figure 6B, in cellular lysates, the *c-fms* mRNA was dramatically enriched in HuR IP samples compared to that in control IgG IP samples. The association of *c-fms* mRNA with HuR was 5.8-fold higher than that seen in the control IgG IP reaction (Fig. 6B, $n = 3$). In contrast, the association of *HMGXB3* mRNA with HuR was not observed (Fig. 6C, $n = 3$), indicating HuR does not directly associate with *HMGXB3* mRNA.

Since HuR stabilizes *c-fms* mRNA (Woo et al. 2009), we checked whether *c-fms* mRNA stabilization down-regulates *HMGXB3* expression. HuR overexpression down-regulates *HMGXB3* expression (Fig. 6D–F; Supplemental Fig. S6A–F, $n = 4$). As expected, *c-fms* expression is up-regulated by HuR overexpression. In contrast, down-regulation of HuR by shRNA up-regulates *HMGXB3* expression and down-regulates *c-fms* expression.

We conclude that HuR stabilizes both *c-fms* mRNA and *c-fms* mRNA with 3' end extension (which is antisense to *HMGXB3* mRNA 3' end), and as a result, down-regulates *HMGXB3* mRNA expression.

The expression pattern is opposite between *c-fms* and *HMGXB3* proteins in breast cancer

UALCAN data set (<http://ualcan.path.uab.edu/>) (Chandrasekar et al. 2017), a comprehensive web resource for

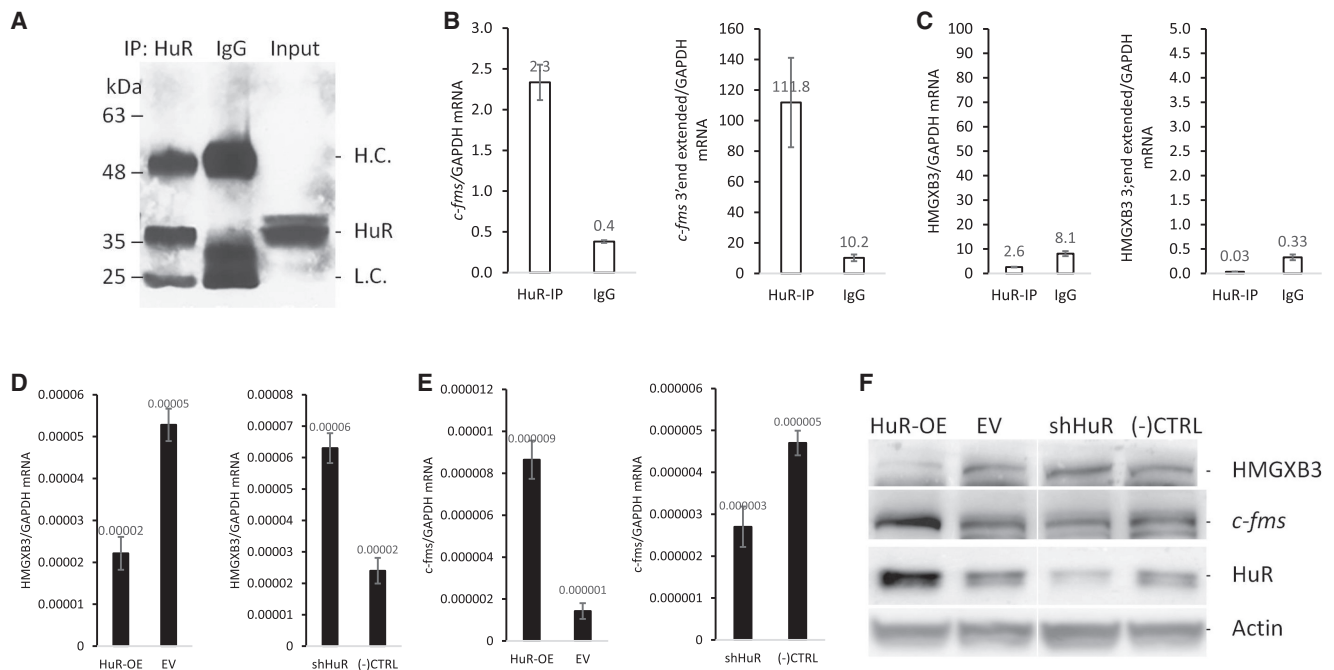


FIGURE 6. HuR targets *c-fms* mRNA, not *HMGXB3* mRNA. (A) HuR IP of BT20 cell lysates. Two-fold excess IgG was used for nonspecific binding. (B) HuR IP enriches *c-fms* mRNA and *c-fms* mRNA with the 3' end extension ($n = 3$), (C) not *HMGXB3* mRNA and *HMGXB3* mRNA with the 3' end extension ($n = 3$). (D) HuR overexpression decreases and shHuR increases *HMGXB3* mRNA ($n = 4$). (E) HuR overexpression increases and shHuR decreases *c-fms* mRNA ($n = 4$). (F) Western analysis shows that HuR overexpression decreases and shHuR increases *HMGXB3* protein. In contrast, HuR overexpression increases and shHuR decreases *c-fms* protein.

analyzing cancer OMICS data, was utilized to identify the protein levels of *c-fms* and HMGXB3 between breast cancer tissues and normal tissues. The UALCAN data analyses indicate that the expression pattern between *c-fms* and HMGXB3 proteins is opposite, that is, the *c-fms* protein level is lower, and the HMGXB3 protein level is higher in general in breast cancer tissues than normal breast tissue (Fig. 7A,B). HMGXB3 is up-regulated and *c-fms* is down-regulated in samples with infiltrating ductal carcinoma (Fig. 7C,D). Luminal, her2/neu, or triple negative breast cancers (TNBC) all showed high expression of HMGXB3 and low expression of *c-fms* compared with normal breast cancer tissue (Fig. 7E,F). This analysis indicates that the expression pattern is opposite between the two proteins in vivo and supports our in vitro findings.

DISCUSSION

Transcription of the convergent gene pair generates mRNA 3' end polymorphism by RNAPII collision or read-through transcription (Fig. 8; Proudfoot 1989; Dye and Proudfoot 1999; Gullerova and Proudfoot 2008; Richard

and Manley 2009; Pelechano et al. 2013; de Klerk and 't Hoen 2015; Kainov et al. 2016). The sense-antisense RNA pair generated by convergent transcription can modulate the expression of mRNA on a posttranscriptional level (PTGS) (Borsani et al. 2005; Kim and Nam 2006; Carthew and Sontheimer 2009; Pelechano and Steinmetz 2013) as well as transcriptional level (TGS) by establishing a local epigenetic imprint (Buhler and Moazed 2007; Gullerova and Proudfoot 2012). NAT generated by convergent transcription also masks sense mRNA and hinders protein-RNA interaction resulting in translation inhibition and RNA decay (Lapidot and Pilpel 2006; Zhang et al. 2006; Pelechano and Steinmetz 2013). The *c-fms* and HMGXB3 convergent gene pair generates mRNA 3' end polymorphism (Figs. 1, 2) resulting in sense-antisense RNA pairing, which regulates their own expression (Figs. 3–6).

Even though both *c-fms* and HMGXB3 mRNAs have conserved poly(A) signal sequences which reside right upstream of the normal termination site, that is, AUUAAA (3963–3968) for *c-fms* mRNA and AAUAAA (5240–5245) for HMGXB3 mRNA (Fig. 8), a small portion of transcripts extends further downstream generating mRNAs with the

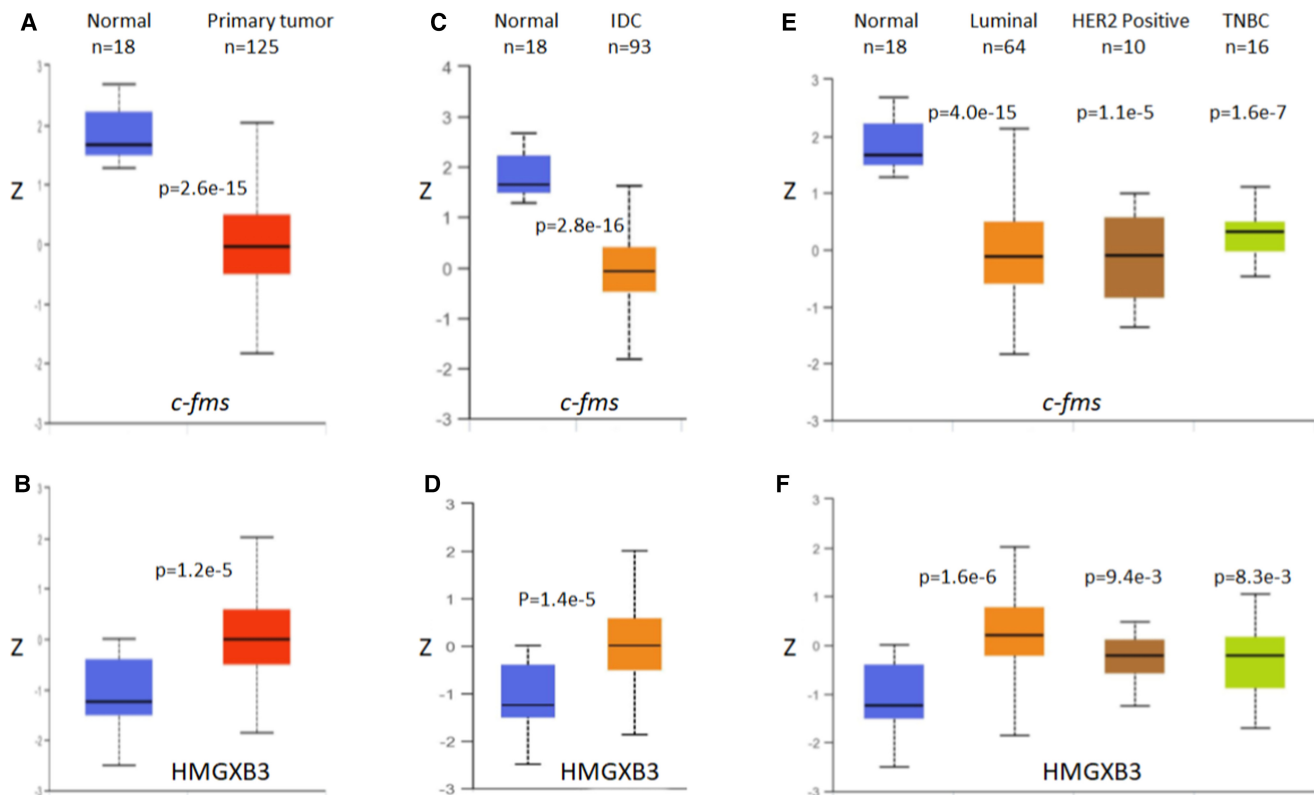


FIGURE 7. The protein expression of *c-fms* and HMGXB3 in breast cancer (UALCAN). (A) The expression of *c-fms* protein in breast cancer tissues is lower than that in normal tissues. (B) In contrast, the expression of HMGXB3 protein in breast cancer tissues is higher than that in normal tissues. (C,D) Similar trends are shown in histologic subtypes, and (E,F) breast cancer subclasses. Z-values on the y-axis represent standard deviations from the median across samples for the given cancer type. Log₂ spectral count ratio values from CPTAC were first normalized within each sample profile, then normalized across samples. P-value less than 0.05 indicates significant differences between samples. (IDC) Infiltrating ductal carcinoma, (TNBC) triple negative breast cancer.

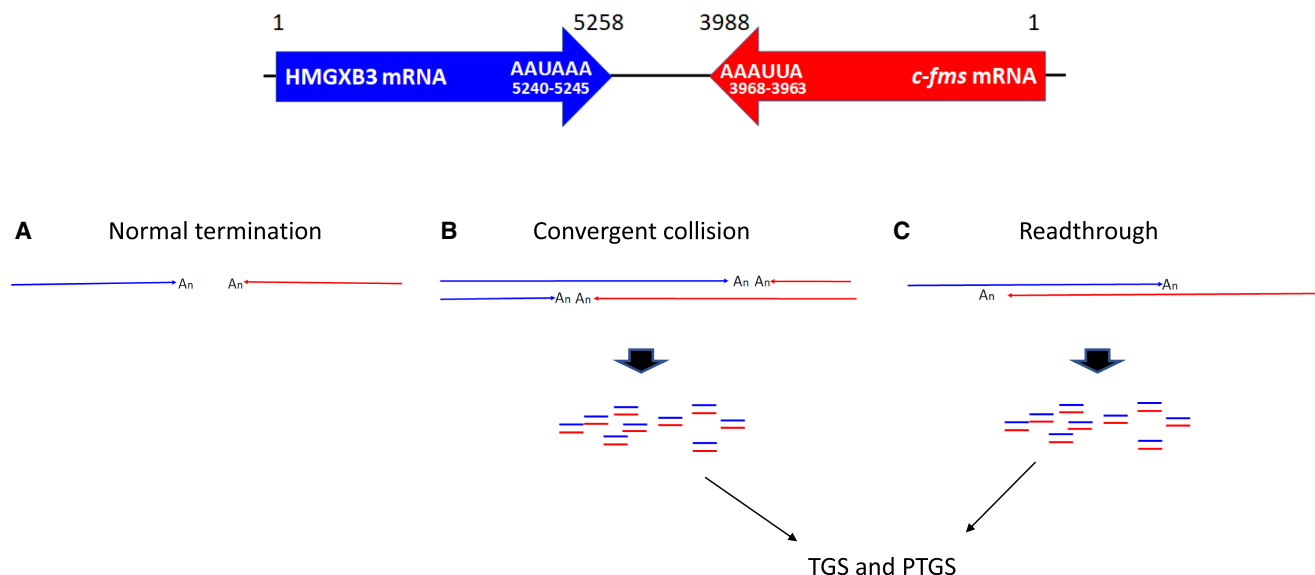


FIGURE 8. Termination of convergent transcription elongation. (A) Transcription elongation complexes collide in the convergent gene pairs and terminate transcription. (B) Differential rate of transcription elongation between the convergent gene pairs results in the 3' end polymorphism. (C) Transcriptional bypass also generates the 3' end polymorphism. mRNA is depicted with the poly(A_n) tail. Poly(A) signal sequences are shown in *HMGXB3* mRNA (5240–5245) and *c-fms* mRNA (3963–3968).

3' end extensions, which serve as natural antisense RNAs (Figs. 1, 2). Furthermore, these *c-fms* and *HMGXB3* mRNAs with the 3' end extensions are still polyadenylated at the 3' end (Fig. 2A). We do not find any specific sequence or structure for termination of extended transcription. We propose that RNAPII collision in convergent gene pair may randomly stop the transcription generating mRNA 3' end polymorphism. The mechanism(s) are unknown at this time. There is a limit to RT-PCR mapping for determination of the exact transcription termination sites and the presented mapping (Fig. 2A) is the most representative. In the future, mRNA 3' end transcriptome NGS needs to be done for accurate mapping and finding the population of variable ends of transcripts.

Knock-in of a strong poly(A) signal (SV40-PA) reduces bidirectional mRNA 3' end extension, thereby reducing sense-antisense RNA pairing, and up-regulating both *c-fms* and *HMGXB3* mRNA and protein expression (Fig. 3). The orientation of poly(A) signal sequence may also contribute to the efficiency of transcription termination. The SV40-PA is introduced in the 5'-to-3' orientation to the end of *HMGXB3* mRNA (Fig. 3), which results in dramatic down-regulation of *HMGXB3* mRNA with the 3' end extension (which is antisense RNA against *c-fms* mRNA) (Fig. 3B) resulting in a profound increase of *c-fms* mRNA (Fig. 3E) and protein (Fig. 3F). The extension of 3' UTRs from both *c-fms* and *HMGXB3* can cause a partial overlap in 3' UTR regions, generating sense-antisense RNA pair resulting in either PTGS or TGS. The length of the overlapping region may be inversely correlated to the level of expression; that is, an increase of *HMGXB3* mRNA (Fig. 3E) and protein

(Fig. 3F) is not comparable with the dramatic increase of *c-fms* expression. Transcription termination of *c-fms* and *HMGXB3* mRNAs may also occur at different time points or simultaneously in the cell.

The miR-324-5p and HuR studies indicate that the major effect of sense-antisense RNA pairs on reduction of mRNA and protein expression is largely on the basis of mRNA instability (Figs. 4–6). miR-324-5p and HuR effects are indirect on either *c-fms* or *HMGXB3* mRNA expression, respectively. miR-324-5p down-regulates *HMGXB3* mRNA and, as a result, increases *c-fms* mRNA (Fig. 4). In contrast, HuR up-regulates *c-fms* mRNA and, as a result, down-regulates *HMGXB3* mRNA (Fig. 6).

Overexpression of *c-fms* mRNA and protein in breast cancer epithelium, including activated phosphorylated *c-fms* protein, has been observed both in vitro and in vivo (Kacinski et al. 1991; Sapi et al. 1995; Flick et al. 1997). Breast cancer tissues, analyzed in the CPTAC/TCGA projects (<http://ualcan.path.uab.edu/>) (Chandrashekar et al. 2017), comprise malignant breast epithelium and its surrounding stroma. In addition, the “normal” breast tissue is frequently collected adjacent to the tumor. This tissue too, contains both epithelium and stroma. The stroma contains many elements, including *c-fms* expressing tumor associated macrophages, which are active players in the breast tumor microenvironment (Lin et al. 2001). It has been shown that the “normal” tissue adjacent to the breast tumor can be an active tumor microenvironment which can portend more impact on prognosis than the breast epithelium itself (Huang et al. 2016). Lastly, detection of activated phosphorylated, *c-fms* protein, requires strict tissue

collection processes. All these factors help explain the finding that *c-fms* protein expression detected in this way was down-regulated in breast cancer tissues compared to “normal” tissues. What is clear from this analysis, however, is that under the same conditions, HMGXB3 protein levels in breast cancer tissues were increased compared to the “normals” (Fig. 7). This analysis of *in vivo* breast tissues, showing that *c-fms* and HMGXB3 expression patterns are opposite, is in line with our *in vitro* findings regarding the existence and implications of *c-fms* and HMGXB3 convergent gene transcription in breast cancer cells.

In conclusion, we are the first to report that *c-fms* and HMGXB3 mRNA 3' end polymorphism is derived from the extended transcription termination, with the intergenic region between *c-fms* and HMGXB3 genes of 162 bp. These *c-fms* and HMGXB3 mRNAs with the 3' end extensions, have poly(A)⁺ tails, and represent 1–4% of total *c-fms* and HMGXB3 mRNAs.

The closely juxtaposed *c-fms* and HMGXB3 gene pair generates extended 3' end transcripts, which form sense-antisense RNA pairs regulating each other's expression.

We find that miR-324-5p, via targeting HMGXB3 3' UTR mRNA, up-regulates *c-fms* expression; while HuR, via interaction and stabilization of *c-fms* mRNA, down-regulates HMGXB3 expression. These sense-antisense RNA pairs result in reduction of mRNA and protein expression largely on the basis of mRNA instability. Lastly, knock-in of a strong poly(A) signal abolishes bidirectional mRNA 3' end extension, thereby reducing sense-antisense RNA pairing, up-regulating both *c-fms* and HMGXB3 mRNA and protein expression.

For future studies, it will be important to explore how *c-fms* and HMGXB3 sense-antisense RNA pair is processed to siRNA to induce gene silencing. In TGS, the RNA binding protein vigilin, which binds pyrimidine-rich sequence in *c-fms* mRNA 3' UTR (Woo et al. 2011), may play a role as it has been reported to induce heterochromatin formation (Zhou et al. 2008).

MATERIALS AND METHODS

Cell culture

BT20 breast cancer cells were cultured in MEM supplemented with 10% fetal bovine serum.

Northern analysis

Total cellular RNA was extracted using TRIzol (Invitrogen). Ten micrograms total RNA was fractionated in 1% agarose-formaldehyde gel and blotted to Hybond-N nylon membrane (Amersham). ³²P-UTP labeled *c-fms* and HMGXB3 strand-specific antisense RNA probes were generated as described in Supplemental Figure S1. Briefly, either *c-fms* (Woo et al. 2009)

or HMGXB3 (in this work) DNA was PCR amplified and the 3' end was tagged with T7 RNA polymerase promoter. *In vitro* transcription was performed with ³²P-UTP and T7 RNA polymerase to synthesize the ³²P-labeled strand-specific antisense RNA probe. After *in vitro* transcription, DNase I was treated to remove DNA template. Northern hybridization was done in 0.75 M NaCl, 10× Denhardt's (0.2% w/v Ficoll, 0.2% w/v Polyvinylpyrrolidone, 0.2% BSA), 50% formamide, and ³²P-labeled antisense RNA probe (2 × 10⁷ cpm/mL) at 42°C, overnight. The membrane was washed in 2× SSC (0.3 M NaCl, 30 mM sodium citrate) and 0.1% SDS at room temperature, and 0.1× SSC and 0.1% SDS at 65°C, 60 min. The membrane was exposed on a storage phosphor screen (GE Healthcare) up to 96 h before image capture by Typhoon FLA7000 Biomolecular Imager (GE).

A list of primers is presented in Supplemental Table S1.

mRNA 3' end mapping

Poly(A)⁺-RNA from BT20 cells was purified using 5'-biotin-linked oligo-dT₂₅ and Dynabeads MyOne Streptavidin C1 (Invitrogen). A total of 10 ng poly(A)⁺-RNA was reverse transcribed with RT primers by M-MuLV Reverse Transcriptase (NEB) and PCR amplified by *Pfu* Polymerase (Promega) as described in detail in Supplemental Figure S2. PCR products were purified by Monarch PCR & DNA Cleanup Kit (NEB) and sequenced to confirm 3' end extension.

A list of RT and PCR primers is presented in Supplemental Table S1.

Quantification of mRNA with 3' end extension

RNA quantification is described in detail in Supplemental Figure S2.

Briefly, 10 ng poly(A)⁺-RNA was reverse transcribed in a reaction tube with three sequence-specific RT primers; that is, RT primer 1 or 4 from *c-fms* or HMGXB3 mRNA coding region, RT primer 2 or 5 from *c-fms* or HMGXB3 mRNA 3' end extension, and RT primer 3 from GAPDH mRNA. RT transcripts were real-time PCR amplified with sybrgreen for quantification as described in Supplemental Figure S2.

A list of primers is presented in Supplemental Table S1.

SV40-PA knock-in by CRISPR/Cas9

To construct the plasmid used in the SV40-PA knock-in (KI), DNA sequences for the left homology arm and right homology arm of targeted *c-fms* and HMGXB3 genes were cloned into the pDonor-D01 (GeneCopoeia). sgRNA-pCas-Guide-EF1a-GFP was generated (Origene).

The following two sgRNAs were used for knock-in that targeted the 5' and 3' regions in IR.

sgRNA 1—AATTCCGTGCACATCGTATG
sgRNA 2—GGAATTTGCAGGTACTCATG

To obtain the *c-fms*-SV40-PA-HMGXB3-KI BT20 cell lines, 3 × 10⁶ cells per well were seeded in a six-well plate with MEM supplemented with 10% fetal bovine serum at 37°C, 5% CO₂. The following day, transfection was carried out with Fugene (Promega).

One day later, puromycin (1 µg/mL) was added to the cells to increase the KI efficiency. Within ~2 wk, positive single colonies were picked up and transferred into 24-well plates. Briefly, genomic DNA was isolated. A total of 100 ng genomic DNA was used as a template for a PCR, and the PCR products were analyzed by Sanger sequencing (Supplemental Fig. S3A).

RNA half-life

To determine *c-fms* and HMGXB3 mRNA half-life in BT20 breast cancer cells, actinomycin-D (Act-D) chase experiments were performed with 5 µg/mL of Act D (Sigma) added to inhibit new transcription. Cells were harvested at 0, 2, 4, 8, and 24 h after Act D treatment, and total cellular RNA was extracted using TRIzol (Invitrogen). qRT-PCR was performed.

c-fms and HMGXB3 mRNA half-lives were calculated after qRT-PCR, normalized to GAPDH mRNA, values were plotted, and the time period required for a given transcript to decrease to one-half of the initial abundance was calculated. GAPDH mRNA is not affected by miR-324-5p and has a long half-life (>18 h) (Woo et al. 2009). Three independent experiments were performed.

Gain-of-function and loss-of-function assays of miR-324-5p

Either hsa-miR-324-5p Mimic (Sigma HMI0479) or hsa-miR-324-5p Inhibitor (Sigma HSTUD0479) was transfected using MISSION siRNA Transfection Reagent (Sigma S1452) for 2 d. For negative control, MISSION miRNA, Negative Control (Sigma HMC0002) was transfected.

Luciferase reporter assay

Firefly luciferase Mut E in pcDNA3.1(–) was obtained from Robert J. Gillies (University of Arizona) (Baggett et al. 2004). Firefly luciferase Mut E fused with *c-fms* mRNA full length 3' UTR (+3212~+3988) without 3' end extension or HMGXB3 mRNA full length 3' UTR (+4323~+5258) without 3' end extension was constructed as described in Supplemental Figure S5.

For luciferase analysis, BT20 cells were transiently cotransfected using Fugene HD (Roche) with firefly luciferase-*c-fms* or HMGXB3 mRNA 3' UTR plasmid and Renilla luciferase control plasmid (Promega). Dual luciferase-activity assays were performed 48 h after transfection according to the manufacturer's directions (Promega). Firefly luciferase activity was normalized by Renilla luciferase. Firefly and Renilla luciferase mRNAs, and GAPDH mRNA were measured by qRT-PCR. Firefly luciferase mRNA was normalized by Renilla luciferase mRNA, and followed by GAPDH mRNA.

RNA capture by immunoprecipitation

The BT20 cell was treated by formaldehyde for RNA–protein crosslink. Immunoprecipitation (IP) of the endogenous mRNP complex was done by the protocol described previously (Woo and Chambers 2019). For HuR IP, 5 µg mouse monoclonal anti-human HuR antibody (Santa Cruz, sc-5261) was used. A reaction containing 10 µg normal mouse IgG (Sigma) served as a negative

control. For immunoblot, cytoplasmic protein was isolated using NE-PER nuclear and cytoplasmic extraction reagents (Thermo Fisher Scientific). Immunoblot was done with HuR antibody (Santa Cruz, sc-365816). For RNA isolation, IP material is digested by proteinase K for 30 min at 55°C, following phenol:CHCl₃ extraction, and ethanol precipitation.

HuR overexpression and silencing in BT20 cells

HuR-pcDNA3.1 (Woo et al. 2009) was transfected for overexpression. For silencing, HuR shRNA (Origene, TI352933) was transfected using Fugene HD (Roche).

UALCAN analysis

UALCAN website (<http://ualcan.path.uab.edu>) is a comprehensive web resource for analyzing cancer OMICS data (Chandrashekar et al. 2017). We utilized this website to explore the protein expression of *c-fms* (i.e., CSF-1R) and HMGXB3 in breast cancer tissues, previously characterized by CPTAC in normal and malignant breast tissues from sources including the TCGA project.

Statistical analysis

Data are depicted as mean ± SD from at least three independent experiments. Exact *n* values are provided in the figure legends. The unpaired two-way *t*-test, nonlinear regression analysis, and one-way ANOVA were performed using SigmaStat (Jandel Scientific Corp.). *P* < 0.05 was considered statistically significant.

SUPPLEMENTAL MATERIAL

Supplemental material is available for this article.

ACKNOWLEDGMENTS

This work was supported by Women's Cancers of the University of Arizona Cancer Center and the Bobbi Olson Endowment Fund (to S.K.C.).

Received March 8, 2021; accepted June 16, 2021.

REFERENCES

- Baggett B, Roy R, Momen S, Morgan S, Tist L, Morse D, Gillies RJ. 2004. Thermostability of firefly luciferase affects efficiency of detection by in vitro bioluminescence. *Mol Imaging* **3**: 324–332. doi:10.1162/1535350042973553
- Borsani O, Zhu J, Verslues PE, Sunkar R, Zhu JK. 2005. Endogenous siRNAs derived from a pair of natural *cis*-antisense transcripts regulate salt tolerance in *Arabidopsis*. *Cell* **123**: 1279–1291. doi:10.1016/j.cell.2005.11.035
- Buhler M, Moazed D. 2007. Transcription and RNAi in heterochromatic gene silencing. *Nat Struct Mol Biol* **14**: 1041–1048. doi:10.1038/nsmb1315
- Carthew RW, Sontheimer EJ. 2009. Origins and mechanisms of miRNAs and siRNAs. *Cell* **136**: 642–655. doi:10.1016/j.cell.2009.01.035

- Chambers SK, Kacinski BM, Ivins CM, Carcangiu ML. 1997. Overexpression of epithelial CSF-1 and CSF-1 receptor: a poor prognostic factor in epithelial ovarian cancer; contrasted to a protective effect of stromal CSF-1. *Clin Cancer Res* **3**: 999–1007.
- Chandrashekar DS, Basher B, Balasubramanya SAH, Creighton CJ, Ponce-Rodriguez I, Chakravarthi BVSK, Varambally S. 2017. UALCAN: a portal for facilitating tumor subgroup gene expression and survival analyses. *Neoplasia* **19**: 649–658. doi:10.1016/j.neo.2017.05.002
- Chen J, Sun M, Kent WJ, Huang X, Xie H, Wang W, Zhou G, Shi RZ, Rowley JD. 2004. Over 20% of human transcripts might form sense-antisense pairs. *Nucleic Acids Res* **32**: 4812–4820. doi:10.1093/nar/gkh818
- Danckwardt S, Hentze MW, Kulozik AE. 2008. 3' end mRNA processing: molecular mechanisms and implications for health and disease. *EMBO J* **27**: 482–498. doi:10.1038/sj.emboj.7601932
- de Klerk E, 't Hoen PAC. 2015. Alternative mRNA transcription, processing, and translation: insights from RNA sequencing. *Trends Genet* **31**: 128–139. doi:10.1016/j.tig.2015.01.001
- Di Giammartino DC, Nishida K, Manley JL. 2011. Mechanisms and consequences of alternative polyadenylation. *Mol Cell* **43**: 853–866. doi:10.1016/j.molcel.2011.08.017
- Dye MJ, Proudfoot NJ. 1999. Terminal exon definition occurs cotranscriptionally and promotes termination of RNA polymerase II. *Mol Cell* **3**: 371–378. doi:10.1016/s1097-2765(00)80464-5
- Faghihi MA, Wahlestead C. 2009. Regulatory roles of natural antisense transcripts. *Nat Rev Mol Cell Biol* **10**: 637–643. doi:10.1038/nrm2738
- Flick MB, Sapi E, Perrotta PL, Maher MG, Halaban R, Carter D, Kacinski BM. 1997. Recognition of activated CSF-1 receptor in breast carcinomas by a tyrosine 723 phosphospecific antibody. *Oncogene* **14**: 2553–2561. doi:10.1038/sj.onc.1201092
- Gullerova M, Proudfoot NJ. 2008. Cohesin complex promotes transcriptional termination between convergent genes in *S. pombe*. *Cell* **132**: 983–995. doi:10.1016/j.cell.2008.02.040
- Gullerova M, Proudfoot NJ. 2012. Convergent transcription induces transcriptional gene silencing in fission yeast and mammalian cells. *Nat Struct Mol Biol* **19**: 1193–1201. doi:10.1038/nsmb.2392
- Guo S, Wang Y, Gao Y, Zhang Y, Chen M, Xu M, Hu L, Jing Y, Li C, Wang Q, et al. 2016. Knockdown of high mobility group-box 3 (HMGB3) expression inhibits proliferation, reduces migration, and affects chemosensitivity in gastric cancer cells. *Med Sci Monit* **22**: 3951–3960. doi:10.12659/msm.900880
- Hans H, Alwine JC. 2000. Functionally significant secondary structure of the simian virus 40 late polyadenylation signal. *Mol Cell Biol* **20**: 2926–2932. doi:10.1128/mcb.20.8.2926-2932.2000
- Hobson DJ, Wei W, Steinmetz LM, Svejstrup JQ. 2012. RNA polymerase II collision interrupts convergent transcription. *Mol Cell* **48**: 365–374. doi:10.1016/j.molcel.2012.08.027
- Huang X, Stern DF, Zhao H. 2016. Transcriptional profiles from paired normal samples offer complementary information on cancer patient survival – evidence from TCGA Pan-Cancer data. *Sci Rep* **6**: 20567. doi:10.1038/srep20567
- Kacinski BM, Carter D, Mittal K, Kohorn EI, Bloodgood RS, Donahue J, Donofrio L, Edwards R, Schwartz PE, Chambers JT, et al. 1988. High level expression of *fms* proto-oncogene mRNA is observed in clinically aggressive human endometrial adenocarcinomas. *Int J Radiat Oncol Biol Phys* **15**: 823–829. doi:10.1016/0360-3016(88)90113-7
- Kacinski BM, Carter D, Mittal K, Yee LD, Scata KA, Donofrio L, Chambers SK, Wang KI, Yang-Feng T, Rohrschneider LR, et al. 1990. Ovarian adenocarcinomas express *fms*-complementary transcripts and *fms* antigen, often with coexpression of CSF-1. *Am J Pathol* **137**: 135–147.
- Kacinski BM, Scata KA, Carter D, Yee LD, Sapi E, King BL, Chambers SK, Jones MA, Pirro MH, Stanley ER, et al. 1991. FMS (CSF-1 receptor) and CSF-1 transcripts and protein are expressed by human breast carcinomas in vivo and in vitro. *Oncogene* **6**: 941–952.
- Kainov YA, Aushev VN, Naumenko SA, Tchevkina EM, Bazykin GA. 2016. Complex selection on human polyadenylation signals revealed by polymorphism and divergence data. *Genome Biol Evol* **8**: 1971–1979. doi:10.1093/gbe/evw137
- Kim VN, Nam JW. 2006. Genomics of microRNA. *Trends Genet* **22**: 165–173. doi:10.1016/j.tig.2006.01.003
- Kuehner JN, Pearson EL, Moore C. 2011. Unravelling the means to an end: RNA polymerase II transcription termination. *Nat Rev Mol Cell Biol* **12**: 1–12. doi:10.1038/nrm3098
- Lapidot M, Pilpel Y. 2006. Genome-wide natural antisense transcription: coupling its regulation to its different regulatory mechanisms. *EMBO J* **7**: 1216–1222. doi:10.1038/sj.embor.7400857
- Lin EY, Nguyen AV, Russell RG, Pollard JW. 2001. Colony-stimulating factor 1 promotes progression of mammary tumors to malignancy. *J Exp Med* **193**: 727–740. doi:10.1084/jem.193.6.727
- Ma N, McAllister WT. 2009. In a head-on collision, two RNA polymerases approaching one another on the same DNA may pass by one another. *J Mol Biol* **391**: 808–812. doi:10.1016/j.jmb.2009.06.060
- Maher MG, Sapi E, Turner B, Gumbs A, Perrotta PL, Carter D, Kacinski BM, Haffty BG. 1998. Prognostic significance of colony-stimulating factor receptor expression in ipsilateral breast cancer recurrence. *Clin Cancer Res* **4**: 1851–1856.
- Nourse J, Spada S, Danckwardt S. 2020. Emerging roles of RNA 3'-end cleavage and polyadenylation in pathogenesis, diagnosis and therapy of human disorders. *Biomolecules* **10**: 915. doi:10.3390/biom10060915
- Ogorodnikov A, Kargaplova Y, Danckwardt S. 2016. Processing and transcriptome expansion at the mRNA 3' end in health and disease: finding the right end. *Pflugers Arch Eur J Physiol* **468**: 993–1012. doi:10.1007/s00424-016-1828-3
- Pelechano V, Steinmetz LM. 2013. Gene regulation by antisense transcription. *Nat Rev Genet* **14**: 880–893. doi:10.1038/nrg3594
- Pelechano V, Wei W, Steinmetz LM. 2013. Extensive transcriptional heterogeneity revealed by isoform profiling. *Nature* **497**: 127–131. doi:10.1038/nature12121
- Proudfoot NJ. 1989. How RNA polymerase II terminates transcription in higher eukaryotes. *Trends Biochem Sci* **14**: 105–110. doi:10.1016/0968-0004(89)90132-1
- Proudfoot NJ. 2016. Transcriptional termination in mammals: stopping the RNA polymerase II juggernaut. *Science* **352**: aad9926. doi:10.1126/science.aad9926
- Richard P, Manley JL. 2009. Transcription termination by nuclear RNA polymerase. *Genes Dev* **23**: 1247–1269. doi:10.1101/gad.1792809
- Sapi E, Flick MB, Gilmore-Hebert M, Rodov S, Kacinski BM. 1995. Transcriptional regulation of the *c-fms* (CSF-1R) proto-oncogene in human breast carcinoma cells by glucocorticoids. *Oncogene* **10**: 529–542.
- Schek N, Cooke C, Alwine JC. 1992. Definition of the upstream efficiency element of the simian virus 40 late polyadenylation signal by using in vitro analyses. *Mol Cell Biol* **12**: 5386–5393. doi:10.1128/mcb.12.12.5386
- Sing M, Wang B, Feng G, Duan L, Yuan S, Jia W, Liu Y. 2019. Knockdown of high mobility group box 3 impairs cell viability and colony formation but increases apoptosis in A549 human non-small cell lung cancer cells. *Oncol Lett* **17**: 2937–2945. doi:10.3892/ol.2019.9927
- Sinturel F, Navickas A, Wery M, Describes M, Morillon A, Torchet C, Benard L. 2015. Cytoplasmic control of sense-antisense mRNA pairs. *Cell Rep* **12**: 1853–1864. doi:10.1016/j.celrep.2015.08.016

- Song N, Wang B, Feng G, Duan L, Yuan S, Jia W, Liu Y. 2019. Knockdown of high mobility group box 3 impairs cell viability and colony formation but increases apoptosis in A549 human non-small cell lung cancer cells. *Oncol Lett* **17**: 2937–2945. doi:10.3892/ol.2019.9927
- Sun LN, Xing C, Zhi Z, Liu Y, Chen LY, Shen T, Zhou Q, Liu YH, Gan WJ, Wang JR, et al. 2017. Dicer suppresses cytoskeleton remodeling and tumorigenesis of colorectal epithelium by miR-324-5p mediated suppression of HMGXB3 and WASF-2. *Oncotarget* **8**: 55776–55789. doi:10.18632/oncotarget.18218
- Toy EP, Chambers JT, Kacinski BM, Flick MB, Chambers SK. 2001. The activated macrophage colony-stimulating factor (CSF-1) receptor as a predictor of poor outcome in advanced epithelial ovarian carcinoma. *Gynecol Oncol* **80**: 194–200. doi:10.1006/gyno.2000.6070
- Werner A, Sayer JA. 2009. Naturally occurring antisense RNA: function and mechanisms of action. *Curr Opin Nephrol Hypertens* **18**: 343–349. doi:10.1097/MNH.0b013e32832cb982
- West S, Proudfoot NJ, Dye MJ. 2008. Molecular dissection of mammalian RNA polymerase II transcriptional termination. *Mol Cell* **29**: 600–610. doi:10.1016/j.molcel.2007.12.019
- Woo HH, Chambers SK. 2019. Human ALKBH3-induced m¹A demethylation increases the CSF-1 mRNA stability in breast and ovarian cancer cells. *Biochim Biophys Acta Gene Regul Mech* **1862**: 35–46. doi:10.1016/j.bbagr.2018.10.008
- Woo HH, Zhou Y, Yi X, David CL, Zheng W, Gilmore-Hebert M, Kluger HM, Ulukus EC, Baker T, Stoffer JB, et al. 2009. Regulation of non-AU-rich element containing *c-fms* proto-oncogene expression by HuR in breast cancer. *Oncogene* **28**: 1176–1186. doi:10.1038/onc.2008.469
- Woo HH, Yi X, Lamb T, Menzl I, Baker T, Shapiro DJ, Chambers SK. 2011. Posttranscriptional suppression of proto-oncogene *c-fms* expression by vigilin in breast cancer. *Mol Cell Biol* **231**: 215–225. doi:10.1128/MCB.01031-10
- Yelin R, Dahary D, Sorek R, Levanon EY, Goldstein O, Shoshan A, Diber A, Biton S, Tamir Y, Khosravi R, et al. 2003. Widespread occurrence of antisense transcription in the human genome. *Nat Biotechnol* **21**: 379–386. doi:10.1038/nbt808
- Zhang Y, Liu XS, Liu QR, Wei L. 2006. Genome-wide *in silico* identification and analysis of *cis* natural antisense transcripts (*cis*-NATs) in ten species. *Nucleic Acids Res* **34**: 3465–3475. doi:10.1093/nar/gkl473
- Zhou J, Wang Q, Chen LL, Carmichael GG. 2008. On the mechanism of induction of heterochromatin by the RNA-binding protein vigilin. *RNA* **14**: 1773–1781. doi:10.1261/rna.1036308